REMARKS/ARGUMENTS

The Office Action of March 30, 2006, rejected the claims as anticipated in view of a patent to Kim (U.S. 6,091,471) on the ground that liquid crystal cells having an in-plane switching mode inherently include interdigitated electrodes. The Office cited to Tomioka (U.S. 6,682,783) as support for the Office's assertion that liquid crystal cells having an in-plane switching mode inherently include a group of interdigitated electrodes .

Applicants traverse the Office's assertion that liquid crystal cells having an in-plane switching mode inherently include interdigitated electrodes. Applicants submit that it is readily recognized by those of ordinary skill in the art that many different types of liquid crystal cells having an in-plane switching mode without interdigitated electrodes are known. For example, at least the following types of liquid crystal cells have an in-plane switching mode but do not have interdigitated electrodes: (i) surface stabilized ferroelectric liquid crystal display devices, (ii) flexoelectric liquid crystal cell display devices, and (iii) field-controlled anchoring liquid crystal display devices.

Applicants submit herewith a copy of a publication by Clark "Sub-Microsecond Bistable Electro-Optic Switching in Liquid Crystals." Clark discloses a surface stabilized ferroelectric liquid crystal display device that carries out switching of the orientation state of different in-plane directions by electric field manipulation of opposite ferroelectric polarization (e.g., by spontaneous polarization of ferroelectric liquid crystals caused by a vertical electrical field electrode present on an opposing surface which causes a change in orientation state). See, for example, the Abstract of Clark where it is stated that electro-optic effects are obtained from the ferroelectric polarization technique. An interdigitated electrode is not disclosed as an element of the Clark device.

Patel ("Flexoelectric Electro-optics of a Cholesteric Liquid Crystal") proves that other liquid crystal cells having an in-plane switching mode without interdigitated electrodes are

known. The electro-optic effect of the Patel publication is attributed to a flexoelectric effect imparted by an electric field applied perpendicular to a surface. The in-plane switching mode display devices of Patel do not include interdigitated electrodes.

Applicants further provide Jaegemalm ("An Electro-Optic Device Based on Field-Controlled Anchoring of a Nematic Liquid Crystal") as evidence that liquid crystal cells having an in-plane switching mode do not inherently have interdigitated electrodes. Jaegemalm describes a further type of liquid crystal cell having an in-plane switching mode that does not have any interdigitated electrode. The display device of Jaegemalm operates through the application of an electric field applied in a normal orientation to the device surfaces. The field-controlled anchoring liquid crystal display device of Jaegemalm does not have any interdigitated electrode.

Applicants submit that the three publications mentioned above, i.e., Jaegemalm, Patel and Clark, prove that it is readily recognized by those of ordinary skill in the art that a liquid crystal cell having an in-plane switching mode does not inherently include a group of interdigitated electrodes. Thus, the Office's basis for asserting that the Kim prior art inherently discloses an in-plane switching mode liquid crystal cell having a group of interdigitated electrodes is not correct. Because interdigitated electrodes are not inherently present in liquid crystal cells having an in-plane switching mode, the Office has not met its burden in establishing that the presently claimed invention is anticipated by the cited prior art.

Applicants request withdrawal of the rejection under 35 U.S.C. § 102(b).

The Office further asserted that the mechanical rubbing of Kim may provide a low pretilt angle, i.e., almost zero degrees (see page 2, fourth full paragraph of the Office Action of March 30, 2006). Applicants traverse the Office's assertion that mechanical rubbing can

provide a pretilt angle of substantially 0°. The arguments of the July 12, 2005 Amendment are reproduced here in part for convenience.

Applicants submit that it is generally recognized by those of skill in the art that mechanical rubbing cannot provide an alignment layer wherein the pretilt angle is substantially 0°. Applicants previously submitted copies of *J. Appl. Phys.*, 62 4100, 1987 (Geary) and *Jpn. J. Appl. Phys.*, 34 L503, 1995 (Seo) with the Amendment of July 12, 2005 as evidence that mechanical rubbing cannot provide a pretilt angle of substantially 0°.

Geary discloses in section II and in Figure 1(C) that a tilt bias is generated by buffing (e.g., by mechanical rubbing treatment). See, for example, the disclosure on page 4101 first full paragraph, left column and Figures 1(A)-(C) of Geary.

Likewise, Seo discloses in section III that a pretilt angle (e.g., identified as θo) may be generated by mechanical rubbing. In Seo the polymer surface is disclosed to have a tilt angle of 0° before the mechanical rubbing (i.e., where the rubbing strength, RS, is 0). After the rubbing however, a pretilt angle θo is present (see Figure 5(A)-(E)). Thus, Seo discloses that when a surface having a pretilt angle of 0° is subjected to mechanical rubbing, the surface subsequently has a pretilt angle that is not substantially 0°.

Applicants submit that Geary and Seo demonstrate that those of ordinary skill in the art readily recognize that mechanical rubbing cannot provide a pretilt angle of substantially 0°. Therefore, the Office's assertion that the first alignment layer of Figures 14(A)-(C) (e.g., ref. no. 8) has a pretilt angle of almost 0° after mechanical rubbing is not correct.

The Office cited to Figures 14(A)-(C) as support that Kim discloses a device having a pretilt angle of substantially 0°. Applicants note that Figures 14(A)-(C) show pretilt angles with a one-headed arrow. As Applicants have previously argued, it is readily recognized by those of ordinary skill in the art that a one-headed arrow indicates a pretilt angle that is not substantially 0°, in contrast to two-headed arrows which may have a pretilt angle of

substantially 0°. As that this meaning of one-headed and two-headed arrows is generally recognized by those of ordinary skill in the art, Applicants submit herewith two technical publications. Seo ("Effect of the Polymer Tilt Angle for Generation of Pretilt Angle in Nematic Liquid Crystal on Rubbed Polyimide Surfaces"), discloses in Figure 5 the effect of rubbing on a surface. The rubbing direction is indicated in Figure 5 of Seo with an arrow. The arrow corresponds with the direction of the pretilt angle which is also indicated by the symbol θo. Seo demonstrates that the direction of mechanical rubbing corresponds to the orientation of the pretilt angle and, as is readily evident from the drawing of Figure 5 of Seo, is not substantially 0°.

Applicants further draw the Office's attention to the publication by Lien ("UV Modification of Surface Pretilt of Alignment Layers for Multidomain Liquid Crystal Displays"), which shows the effect of rubbing directions on pretilt angle. The pretilt angle of the substrate is demonstrated by a series of parallel hashed lines. The corresponding rubbing directions are represented by the crossed arrows shown as (c). Applicants submit that Lien discloses that pretilt angle corresponds with rubbing direction and that rubbing direction cannot provide a pretilt angle of substantially 0°. Thus, when a rubbing direction is shown, it synonymously represents the direction of the pretilt angle which is not substantially 0°.

It follows that a two-headed arrow indicates a pretilt angle of substantially 0°, e.g., where the direction of the pretilt is equivalent in both directions and accumulative pretilt angle must be substantially 0°.

The Office further cited to column 5, lines 30-32 and Figure 4 of Kim as support for the rejection (see the fourth paragraph on page 2 of the March 30, 2006 Office Action). Applicants note that the disclosure at column 5, lines 30-32 is in reference to Figure 3 of Kim which describes the photo-irradiation of an alignment layer (Reference No. 9) which is present on a substrate (Reference No. 2) shown in Figure 2 of Kim. The photo-irradiation of

Figure 3 of Kim is not carried out on both substrates and both alignment layers of a liquid crystal display device having a pair of substrates. In contrast, the presently claimed invention is drawn to a liquid crystal display device having at least a pair of substrates. Thus, the disclosure at column 5, lines 21-32 and Figures 2-4 of Kim discloses that only one alignment layer and substrate layer are irradiated. This disclosure cannot serve as evidence that the presently claimed invention is anticipated because it does not disclose that both substrates of liquid crystal display device (e.g., a liquid crystal cell) having a pair of substrates are irradiated. The photo-irradiation of Figure 3 is carried out on only one substrate (i.e., Reference No. 2) and only one alignment layer (i.e., Reference No. 9), see Figure 2. Figure 5a shows that a different substrate (i.e., Reference No. 1) and a different alignment layer (i.e., Reference No. 8) are rubbed but are otherwise not exposed to photo-irradiation.

Thus the Office's citation to Figure 4 and/or column 5, lines 30-32 of Kim as evidence that the presently claimed invention is anticipated is factually incorrect.

Applicants submit that the presently claimed invention is not anticipated by Kim as evidenced by at least (i) the fact that the Office cites to disclosure of Kim which does not describe a device having a pair of substrates both of which are irradiated, (ii) mechanical rubbing cannot provide a pretilt angle of substantially 0°, (iii) those of ordinary skill in the art readily recognize that a liquid crystal cell having an in-plane switching mode does not inherently have interdigitated electrodes, and (iv) the one-headed arrows used in the figures of Kim describe pretilt angles that are not substantially 0°.

In view of the foregoing, Applicants submit that the Office's rejection of the present claims is not supportable and should be withdrawn. Applicants request withdrawal of the rejections and the passage of all now-pending claims to Allowance.

Respectfully submitted,

OBLON, SPIVAK, McCLELLAND,
MAIER & NEUSTADT, P.C.
Norman F. Oblon

Stefan U. Koschmieder, Ph.D.
Registration No. 50,238

Customer Number
22850

Tel: (703) 413-3000
Fax: (703) 413 -2220
(OSMMN 03/06)

An electro-optic device based on field-controlled anchoring of a nematic liquid crystal

P. Jägemalm,[a] L. Komitov, and G. Barbero[b]
Department of Microelectronics and Nanoscience, Chalmers University of Technology, 412 96 Göteborg, Sweden

(Received 30 December 1997; accepted for publication 21 July 1998)

A surface-controlled electro-optic device using a nematic liquid crystal enclosed between two thin spaced glass plates is presented. Modulation angles of the optic axis up to more than 70° can be achieved even for small applied voltages. The switching of the optic axis occurs with a large component in the plane of the sample even though the electric field is applied normal to the sample surfaces. The effect seems to be driven by the dielectric coupling of the liquid crystal molecules with the applied electric field. The field induced switching process is governed by the bounding surfaces that have been covered with obliquely evaporated SiO_x. The mechanism of the phenomenon is briefly discussed. © *1998 American Institute of Physics.* [S0003-6951(98)02238-4]

In nematic liquid crystals, the average orientation (**n**) of the long molecular axis of the rod-shaped molecules takes on the properties of a macroscopic optic axis. Since the orientation of the molecules is easily altered with external fields a number of electro-optic devices have been suggested and realized. One of the major applications for liquid crystals is in flat panel displays. Many of these displays have suffered from a limited viewing angle due to the fact that the switching of the molecules (and thus the optic axis) occurs perpendicular to the plane of the display area and the image contrast becomes dependent on the position of the observer. During the last 15 years attention has therefore been focused on techniques where the optic axis can be switched in the plane of the display.[1–3] However, for in-plane switching in nematics the electric field usually has to be applied in the plane of the display which causes problems with resolution and additional costs. One of the techniques suggested for avoiding this problem involves bistable switching of the liquid crystal molecules in a sandwiched cell whose substrates were covered with obliquely evaporated SiO_x.[4,5] In this letter we report on an electro-optic device where the switching is based on the same type of substrates.

Recently a temperature induced anchoring transition in nematic liquid crystals aligned by evaporated SiO_x has been reported.[6,7] It was shown that the molecular orientation in the so-called twofold degenerate alignment is temperature dependent. This type of alignment can be found for a small interval of evaporation angles,[6,8–11] typically in the range of 67°–75°. For higher and lower evaporation angles two uniform monostable types of alignment are found where the molecules lie in the evaporation plane (Σ) and with a certain pretilt ($\mathbf{n}\|\Sigma$, $0°<\theta<90°$, $\phi=0°$) for high evaporation angles and perpendicular to the evaporation plane and with zero pretilt ($\mathbf{n}\perp\Sigma$, $\theta=90°$, $\phi=90°$) for low evaporation angles, (see Fig. 1). Thus, the temperature induced anchoring transition mentioned above can be seen as a continuous transition between these two monostable states. Here, we report on how this anchoring transition is affected by applying an electric field perpendicular to the cell substrates, or in other words the electro-optic response of the cell in the transition region. The remarkable feature of our technique is that even though the field is applied perpendicularly to the cell there is an effective rotation of the optic axis in the plane of the sample. So far, the only similar study that has been performed in this field was presented by Nobili and Durand,[12] but it was performed for samples at the opposite limit of the twofold degenerate (bistable) alignment for another purpose.

The cells used in this study were of the conventional sandwich type consisting of two indium–tin–oxide (ITO) coated glass plates (Baltracon Z20) with alignment layers of obliquely evaporated SiO_x. The SiO_x was evaporated at 8 Å/s to a total thickness of 200 Å (measured perpendicular to the substrate) and at an angle $\alpha=74°$ from the substrate normal. All depositions were carried out at room temperature and in high vacuum (10^{-7} mbar, SiO source). Cells with cell gap $d=3$ and 6 μm were assembled. The nematic liquid crystal material used was E7 (Merck), which has positive

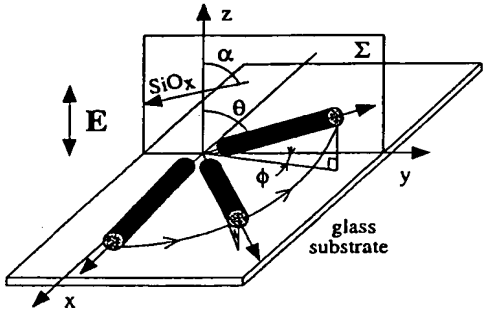

FIG. 1. Schematic representation of the switching of the liquid crystal molecules close to the interface cell substrate (SiO_x)/liquid crystal when an electric field is applied. The SiO_x evaporation plane is represented by Σ, the evaporation angle by α, and the polar and azimuthal angle by θ and ϕ, respectively.

[a]Electronic mail: jagemalm@fy.chalmers.se
[b]Present address: Dipartimento di Fisica and INFM, Politecnico di Torino, 10129 Torino, Italy.

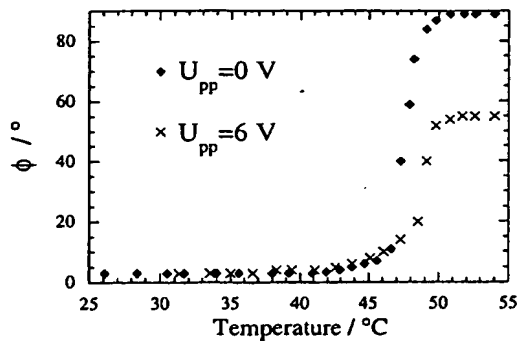

FIG. 2. The effect of an applied electric field (U_{pp}) on the temperature induced reorientation of the optic axis in a cell with the twofold degenerate alignment. Large switching angles can be achieved even for small applied voltages in the high temperature interval. The SiO_x evaporation angle is $\alpha = 74°$.

dielectric anisotropy, $\Delta\epsilon > 0$. The filling of the cells was performed under vacuum and with the liquid crystal material in the isotropic phase. Special attention was paid to the filling process since the selection of molecular orientation is strongly dependent on this process.[13] We were able to obtain textures with only one of the two possible orientations in the twofold degenerate alignment in most of the cells. The investigations of the cell textures were performed in a polarizing microscope (Zeiss Photo microscope II Pol.) equipped with a hot stage (Mettler FP52) for temperature control and with the possibility of applying ac or dc electric fields to the cells.

In a cell with the SiO_x alignment layer evaporated at $\alpha = 74°$ the director is found to be oriented close to the evaporation plane at low temperatures (see Fig. 2). As the temperature increases, the director reorients towards the position perpendicular to the evaporation plane with zero pretilt. (It has been shown that this anchoring transition essentially follows a plane which is tilted about 20° with respect to the substrate.[14] A small hysteresis has then been neglected.[6]) However, if an electric field is applied across the cell, the magnitude of the thermal reorientation of the preferred direction of alignment changes. The reorientation starts approximately at the same temperature independently of the applied voltage while the maximum rotation of the director is significantly smaller with the voltage applied than without (see Fig. 2). The higher the applied voltage is, the smaller the reorientation is. The voltage dependence depicted in Fig. 2 was obtained using an ac voltage of $f = 100$ Hz applied over the transparent ITO electrodes on the two substrates. By switching the electric field on and off, we can thus reorient the director and thereby achieve a large modulation of the azimuthal angle, ϕ, of the optic axis in the high temperature interval. Examples of such measurements are shown in Figs. 3(a) and 3(b) where the *normalized* azimuthal angle $\phi_{norm} = \phi_{max} - \phi(E)$ has been plotted for two cells with a different cell gap as a function of the applied voltage (ϕ_{max} is the maximum azimuthal angle induced by increasing the temperature, $\phi_{max} \approx 89°$). The maximum reorientation of the optic axis is found to be approximately 75°. However, at the high voltages required for these large angles the dielectric coupling with the electric field increases the average molecular tilt from the substrate and thus decreases the birefringence of the sample. The result is a decrease of the contrast. The optical response time is fairly short, about 1 ms in rise time (10→90%) and 1.5 ms in decay time for a pulse of 6 V applied to a cell with a cell gap $d = 6$ μm. The cell texture was homogeneous and the switching occurs over the entire electrode area.

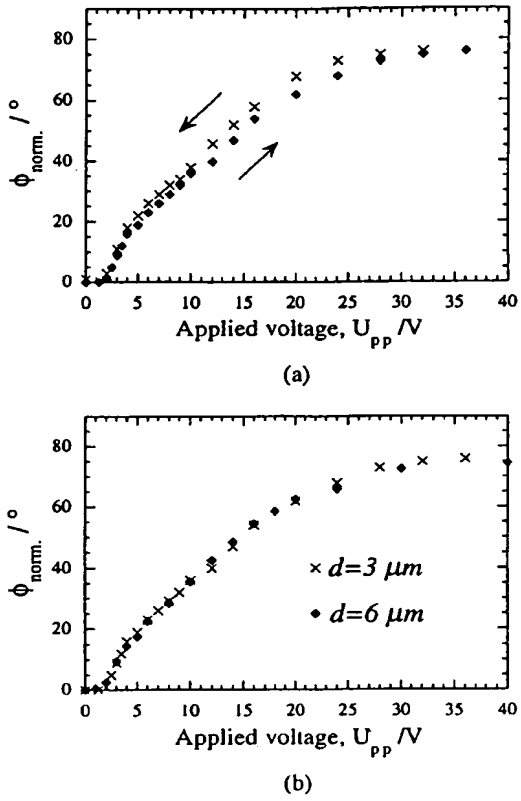

FIG. 3. Normalized azimuthal angle of the optic axis, ϕ_{norm}, as a function of the applied voltage (U_{pp} ac voltage, $f = 100$ Hz, $T \approx 50$ °C). In (a) (cell gap $d = 3$ μm) the small hysteresis found is shown, whereas in (b) a comparison between two cells with cell gap $d = 6$ μm and $d = 3$ μm is shown for increasing T. The evaporation angle is the same as in Fig. 2.

The reorientation of the optic axis shown in Figs. 3(a) and 3(b) has a small but noticeable threshold voltage. This is probably due to the symmetry of the initial nematic orientation and can be described as a Freedericksz transition effect.[15] The critical voltage for reorientation is then given by $V_c = E_c d = \pi\sqrt{k/|\epsilon_a|}$ [independent of cell thickness d, as shown in Fig. 3(b)] which for the nematic material E7 is on the order of 2 V. Above the threshold, the reorientation is almost linear for small applied voltages and then it saturates as the voltage is increased. To describe the effect of an applied electric field along the normal of the sample, $\mathbf{E} = E\mathbf{z}$, we write the total energy per unit surface area of the sample as[16]

$$F(\theta,\phi) = \int_{-d/2}^{d/2} \frac{1}{2} k \left\{ \theta'^2 + \sin^2\theta \phi'^2 \pm \frac{1}{\xi^2} \sin^2\theta \right\} dz + 2F_s(\theta_s, \phi_s), \quad (1)$$

where the sign + holds for positive dielectric anisotropy $\epsilon_a > 0$, and − for $\epsilon_a < 0$. The factor k is the nematic elastic constant (one constant approximation) and $F_s(\theta_s, \phi_s)$ is the

anisotropic part of the surface energy on the substrates at $z = \pm d/2\,[\theta_s = \theta(\pm d/2), \quad \phi_s = \phi(\pm d/2)]$. The term $\xi = \sqrt{k/(|\epsilon_a|E^2)}$ is the electric coherence length and gives an idea of the length over which the effect of the electric field on the director overcomes the orienting effects of the walls. Now, the actual values of $\theta(z)$ and $\phi(z)$ are the ones minimizing $F(\theta,\phi)$ given by Eq. (1). The minimization of Eq. (1) leads to differential equations with belonging boundary conditions. For voltages higher than the critical one, given by the Freedericksz transition described above, it is possible to show[17] that the contribution (F_{el}) from the applied electric field to the surface energy can be taken into account by changing the anisotropic part of the surface energy F_s to an "effective" surface anchoring energy, F_s^{eff}. To model the anisotropic part of the surface energy we make use of a Landau–de Gennes power series expansion which correctly describes the symmetry of the evaporated SiO_x surface.[14] The expansion has been shown to give a good fit of the temperature induced transition[14] where the director reorients on a plane, as described above. Let $p = \cos\theta_s$ and $q = \sin\theta_s \cos\phi_s$, then the surface energy can be expressed as

$$F_s^{\text{eff}}(\theta_s,\phi_s) = \tfrac{1}{2}Ap^2 + \tfrac{1}{4}Bp^4 + \tfrac{1}{2}aq^2 + \tfrac{1}{4}bq^4 + \tfrac{1}{2}cp^2q^2 + F_{\text{el}}, \tag{2}$$

where A, B, a, b, and c are temperature dependent phenomenological parameters. By minimizing the effective surface energy one deduces that[17]

$$(\nu + \eta\cos^2\theta_s)\cos\theta_s = \frac{V}{V_c}$$

and

$$\sin\phi_s = \frac{\sqrt{-[(a/b)+(c/b)\cos^2\theta_s]}}{\sin\theta_s}, \tag{3}$$

where ν, η and a, b, c are free parameters which can be used to fit experimental data and V is the applied voltage. Even though the model is simple and Eq. (3) above does not contain all the details of the reorientation (a more detailed description including simulations of experimental data is in progress[17]), it is evident that an induced change of the polar angle may also lead to a reorientation in the azimuthal direction. The qualitative idea is that the two angles θ and ϕ are coupled[8,6,14] and that the change of the polar angle θ, induced by the coupling with the field, automatically gives rise to a change in the azimuthal angle, at least for the molecules near the surfaces. This is supported by the fact that the model seems to give the most correct predictions when the molecules close to the surfaces are bound to reorient on an imaginary plane, which is characterized by the same parameters as previously used to described the plane for the temperature induced transition.

To conclude, we have presented a device based on an electro-optic effect that involves switching of the optic axis with a large component in the plane of the sample even though the electric field is applied normal to the bounding surfaces. Large switching angles can be achieved for small voltages and the optical response time is short (1 ms for $U_{pp} = 6$ V and $d = 6\ \mu$m). A simple model has been suggested, based on the dielectric coupling of the liquid crystal molecules with the applied electric field. If the temperature range of the twofold degenerate orientation can be extended, this new technique offers a wide potential for applications.

Two of the authors, P. J. and L. K., acknowledge financial support from the Swedish Research Council for Engineering Sciences. They also thank A. K. Zvezdin for fruitful discussions and I. Dierking for comments on the manuscript.

[1] N. A. Clark and S. T. Lagerwall, Appl. Phys. Lett. **36**, 899 (1980).
[2] R. Kiefer, B. Weber, F. Windsceid, and G. Baur, *Proceedings of the 12th International Display Research Conference* (Society for Information Display and the Institute of Television Engineers of Japan, Hiroshima, 1992), p. 547.
[3] M. Oh-e, M. Ohta, S. Aratani, and K. Kondo, *Proceedings of the 15th International Display Research Conference* (Society for Information Display and the Institute of Television Engineers of Japan, Hamamatsu, 1995), p. 557.
[4] R. Barberi and G. Durand, Appl. Phys. Lett. **58**, 2907 (1991).
[5] R. Barberi, M. Giocondo, and G. Durand, Appl. Phys. Lett. **60**, 1085 (1992).
[6] P. Jägemalm and L. Komitov, Liq. Cryst. **23**, 1 (1997).
[7] P. Jägemalm, D. S. Herman, L. Komitov, and F. Simoni, Liq. Cryst. **24**, 335 (1998).
[8] M. Monkade, M. Boix, and G. Durand, Europhys. Lett. **5**, 697 (1988).
[9] M. Monkade, These de Troisieme Cycle, Orsay, France, 1986.
[10] B. Jerome, Boix, and P. Pieranski, Europhys. Lett. **5**, 693 (1988).
[11] R. Barberi, M. Giocondo, M. Iovane, I. Dozov, and E. Polossat, Liq. Cryst. **25**, 23 (1998).
[12] M. Nobili and G. Durand, Europhys. Lett. **25**, 527 (1994).
[13] B. Jerome and P. Pieranski, J. Phys. (France) **49**, 1601 (1988).
[14] P. Jägemalm, G. Barbero, L. Komitov, and A. Strigazzi, Phys. Lett. A **235**, 621 (1997).
[15] V. Freedericksz and V. Zolina, Trans. Faraday Soc. **29**, 919 (1933).
[16] P. G. de Gennes, *The Physics of Liquid Crystals* (Clarendon, Oxford, 1974).
[17] P. Jägemalm, G. Barbero, L. Komitov, and A. K. Zvezdin (unpublished).

Flexoelectric Electro-optics of a Cholesteric Liquid Crystal

J. S. Patel
AT&T Bell Laboratories, Murray Hill, New Jersey 07974

and

Robert B. Meyer
The Martin Fisher School of Physics, Brandeis University, Waltham, Massachusetts 02254
(Received 18 December 1986)

A linear electro-optic effect in a cholesteric liquid crystal is described and attributed to the flexoelectric effect. An electric field applied perpendicular to the helix axis rotates the director about an axis parallel to the field. This produces a periodic splay-bend pattern in the helix, which couples flexoelectrically to the field.

PACS numbers: 61.30.Gd, 78.20.Jq

The helical structure of a cholesteric liquid crystal can be modified or even completely unwound by an applied electric field. This is well understood in terms of the coupling of the electric field to the dielectric anisotropy of the liquid crystal, an effect which is quadratic in the amplitude of the electric field. In this Letter, a new effect is described which is linear in the electric field, and therefore arises from a different coupling mechanism. Following a description of the observations, an explanation is proposed in terms of the linear flexoelectric effect, which accounts for all the experimental observations, and predicts some other properties that can be tested.

The phenomenon is readily observed in a uniformly aligned parallel-plate cell in which the helical axis of the cholesteric lies parallel to the glass surfaces in a unique direction. The inner surfaces of the cell are coated with transparent electrically conductive layers so that an electric field can be applied perpendicular to the plates and to the helix axis. When such a cell is observed between crossed polarizers, extinction is observed whenever the helix axis is parallel or perpendicular to the polarizer, since macroscopically a small-pitch cholesteric acts like a uniaxial crystal with the helix as its optical axis. In this extinction configuration, when a small electric field is applied, the cell transmits light, indicating a rotation of the optical axis in the plane of the cell. By rotation of the cell through a small angle, extinction is once again achieved. It is found that the rotation direction changes with the polarity of the field and the rotation angle is linear in the field amplitude, at least for small fields.

This effect has been observed in several different cholesterics. Figure 1 displays results for *S*-4-*n*-nonyloxyphenyl-4'-(3",7"-dimethyloctyloxybenzoyloxy) benzoate, in a cell approximately 2.75 μm thick and with indium-tin oxide electrodes coated with poly-1,4-butyleneterephthalate to produce parallel molecular alignment at the surface.[1] Initial alignment of the helix axis parallel to the glass was achieved by cooling of the sample from the isotropic state in the presence of an electric field. Because this material has a positive dielectric anisotropy, this orientation of the helix has the lowest dielectric energy. This geometry should produce a fingerprint texture. However, this texture was not visible at low fields, in the material being examined, because of the short pitch comparable to the wavelength of the light. It was nevertheless clearly evident in the presence of an electric field at values close to the unwinding voltage. Measurements of the effect were then made with a 40-Hz square wave of variable amplitude, monitoring the

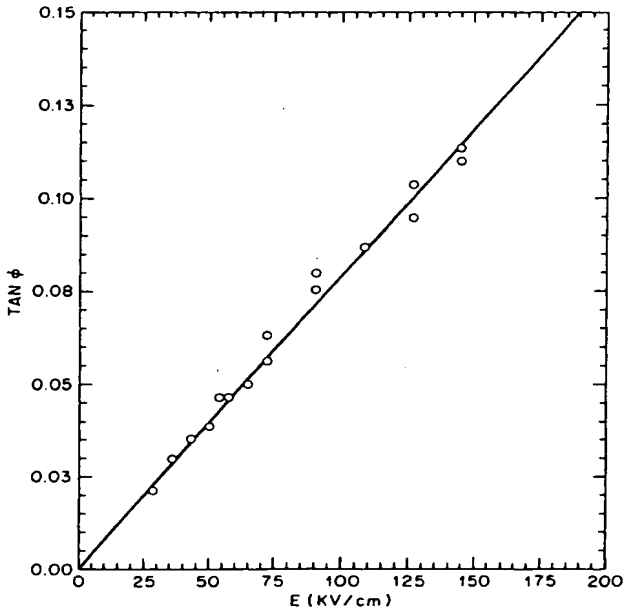

FIG. 1. Rotation of the optical axis (tanϕ) vs applied field (E).

transmitted light intensity with a photodiode and an oscilloscope. For each field amplitude the cell was rotated clockwise and counterclockwise to find the extinction angles for each polarity of field. The dependence of rotation angle on field is linear up to the field at which the dielectric coupling results in unwinding the helix. Although this effect is clearly observed in thicker samples (14 μm), the poor quality of alignment prevented quantitative measurements in these samples for this material.

It is proposed that these observations are explained by the flexoelectric effect, which is a linear coupling between an electric polarization and splay and bend deformations of the liquid crystal. Although the flexoelectric effect has been known and studied for a long time, it has played a secondary role in the phenomenology of liquid crystals because of its complex geometrical requirements. It is most easily observed when either the liquid crystal[2,3] or the electric field[4] is highly inhomogeneous in orientation. The present case is no exception in this regard, although it is simpler in practical respects than other flexoelectric phenomena.

One of the first flexoelectric phenomena proposed by Meyer[5] is one in which a uniform electric field induces the formation of a continuously rotating director structure consisting of alternating bands of splay and bend deformation, as seen in Figs. 2(d) and 2(e). The formation of such a structure from a uniformly aligned nematic has never been observed, for two reasons. First, the flexoelectric effect must compete with ordinary dielectric anisotropy, and the latter coupling usually dominates, maintaining uniform orientation. Second, the continuously rotating director pattern would have to be formed by the generation and movement of defects through the sample, which would occur most easily with high static fields. However, high static fields usually induce electrohydrodynamic instabilities that would obscure the flexoelectric structure.

Starting from the helical cholesteric structure rather than the nematic ground state circumvents these two problems. The director is already continuously rotating in the cholesteric, in a pure twist fashion. It remains only for the flexoelectric effect to modify this structure to introduce components of splay and bend curvature. This is achieved by rotation of the director about an axis parallel to the electric field, as shown in Fig. 2. In both sign and magnitude the splay and bend deformations vary linearly with the rotation angle, at least at small angles. Our understanding of this geometry came partly from the elegant work of Bouligand, among others, who studied cholesteric structures in biological materials such as insect and crab cuticle and dinoflagellate chromosomes.[6] Microtomed specimens in which the slice is taken at an oblique angle to the cholesteric helix axis exhibit the multiply arched pattern of Figs. 2(d) and 2(e).

To make this model quantitative, consider a cholesteric helix in which the director $\hat{\mathbf{n}}$ is parallel to the x-y plane, with $n_x = \cos\theta$ and $n_y = \sin\theta$. In the presence of an electric field $\mathbf{E}$ along the x direction, it is proposed that the helix axis which was initially along the z direction rotates by an angle ϕ about the x axis (in the laboratory frame of reference, the helix axis is fixed for the sample geometry studied, and the x-y plane rotates by $-\phi$). Splay and bend deformations are described by vector fields $\mathbf{S}$ and $\mathbf{B}$, parallel to the x-y plane, given by $\mathbf{S} = \hat{\mathbf{n}}(\nabla\cdot\hat{\mathbf{n}})$ and $\mathbf{B} = \hat{\mathbf{n}}\times\nabla\times\hat{\mathbf{n}}$. Twist is described by $t = \hat{\mathbf{n}}\cdot\nabla\times\hat{\mathbf{n}}$. The free-energy density f for a cholesteric of equilibrium twist t_0 is

$$f = \tfrac{1}{2}\{K_1 S^2 + K_2(t_0 - t)^2 + K_3 B^2\} - e_s \mathbf{E}\cdot\mathbf{S} - e_b \mathbf{E}\cdot\mathbf{B} + (1/8\pi)\epsilon_a E^2 \sin^2\theta, \quad (1)$$

in which the K_i are the splay, twist, and bend elastic constants, e_s and e_b are the splay and bend flexoelectric coefficients, and ϵ_a is the anisotropic part of the dielectric constant.

To see the consequences of the flexoelectric effect in the simplest form, it is assumed that $K_1 = K_3$, $\epsilon_a = 0$, and $e_s = e_b = \bar{e}$, the mean flexoelectric coefficient. If we denote partial derivatives by subscripts, the free-energy

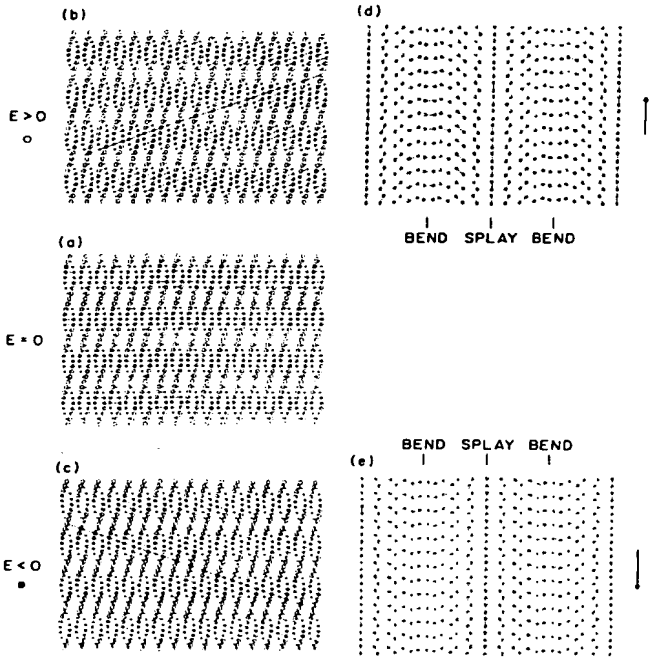

FIG. 2. The helical structure viewed normal to the helix axis, (a) in the absence of an electric field, and (b),(c) in the presence of an electric field perpendicular to the plane of the drawing, which shows the induced director rotation. (d),(e) Cross sections of the helix as indicated by the lines in (b) and (c), displaying the splay-bend pattern.

density reduces to

$$f = \tfrac{1}{2} K_1 \theta_y^2 - \bar{e} E \theta_y + \tfrac{1}{2} K_2 (t_0 - \theta_z)^2. \quad (2)$$

This is clearly minimized by $\theta_z = t_0$ and $\theta_y = \bar{e}E/K_1$. If we denote the rotated helix axis by a wave vector $\mathbf{k}$, with $\theta = \theta_0 + \mathbf{k}\cdot\mathbf{r}$, then $k\cos\phi = t_0$ and $k\sin\phi = \bar{e}E/K_1$. The rotation angle is given by $\tan\phi = \bar{e}E/t_0 K_1$, which is linear in E for small rotations. With use of this expression, and the value of the slope in Fig. 1, it is found that $\bar{e} = 3\times10^{-5}$ cgs units, for $K_1 = K_3 = 1\times10^{-6}$ dyn and helix pitch $= 0.5$ μm. This value is similar to those for other liquid crystals.[4,7] At first it may seem strange that the free energy is lowered by a uniform rotation of the molecules about the electric field direction, but it should be recalled that the flexoelectric coupling induces curvature, not alignment.

A drawback of this simplified theory is that it ignores the dielectric coupling, which distorts and eventually unwinds the helix. It is interesting to determine how the flexoelectric effect influences the helix unwinding field. Still, under the assumption of a uniformly rotated helix axis, the definition of a spatial coordinate h along the helix axis results in $\theta_z = \theta_h \cos\phi$ and $\theta_y = \theta_h \sin\phi$. Let us assume $K_1 = K_3$ to simplify the mathematics without serious loss of generality; then the free energy can be written

$$f = A\theta_h^2 + B\theta_h + C + \tfrac{1}{2} K_2 t_0^2, \quad (3)$$

$$A = \tfrac{1}{2}(K_1 \sin^2\phi + K_2 \cos^2\phi), \quad (4)$$

$$B = (-e_s \cos^2\theta - e_b \sin^2\theta) E \sin\phi - K_2 t_0 \cos\phi, \quad (5)$$

$$C = (1/8\pi)\epsilon_a E^2 \sin^2\theta. \quad (6)$$

This form of free-energy density can be dealt with by the same methods used to understand the unwinding of the helix by the simple dielectric coupling. The first integral of the Euler-Lagrange equation is given by $\theta_h = \pm[(C + Q)/A]^{1/2}$, in which Q is a constant of integration. θ can be written in terms of elliptic integrals. By our substituting this form of θ_h into the mean free energy and minimizing with respect to ϕ and Q, it is possible to derive expressions for the pitch of the helix and the rotation angle ϕ as a function of electric field. Surprisingly, the simple result for $\tan\phi$, derived above, remains valid even in this much more general case.

The critical field E_c for unwinding the helix is, however, modified by the flexoelectric coupling:

$$E_c = \tfrac{1}{2}\pi t_0 [4\pi K_2/(\epsilon_a - \pi^3 \bar{e}^2 K_1^{-1})]^{1/2}. \quad (7)$$

The effective dielectric anisotropy is thus reduced by the flexoelectric effect. Since the flexoelectric coupling tends to keep the director in a helical configuration, it opposes the dielectric coupling, and can substantially increase the critical field over what it would be if $\bar{e}$ were zero.

This prediction can be tested by the study of the frequency dependence of the flexoelectric effect and of the critical field. A remarkable feature of this form of the flexoelectric effect is that a small homogeneous rotation of all the molecules in the system produces a short wavelength periodic splay-bend structure with a small intrinsic relaxation time. In the materials that have been studied, the flexoelectric distortions follow the field up to frequencies of several kilohertz, above which rotational viscosity suppresses the response. At high frequencies therefore the critical field for unwinding the helix should decrease. In the materials that have been tested, the flexoelectric effect has been small enough and the frequency dependence of the dielectric anisotropy large enough to make this experiment ambiguous.

The practical applications of this new effect remain to be explored. To maximize the reponse, it is desirable to have a material which has large flexoelectric coefficients of the same sign, a requirement about which little is known at the level of designing new molecules. To achieve large rotation angles in this effect, it is necessary to avoid the unwinding of the helix by the dielectric coupling, which suggests that the dielectric anisotropy should be small. Eventually this effect may have application as a modulator of optical transmission or optical Bragg scattering.

We are very grateful to J. W. Goodby for stimulating discussions and for providing the liquid-crystalline materials.

[1]J. S. Patel, T. M. Leslie and J. W. Goodby, Ferroelectrics **59**, 129 (1984).

[2]N. V. Madhusudana and G. Durand, J. Phys. (Paris), Lett. **46**, L195 (1985).

[3]G. Durand, Mol. Cryst. Liq. Cryst. **113**, 237 (1984).

[4]J. Prost and P. S. Pershan, J. Appl. Phys. **47**, 2298 (1976).

[5]R. B. Meyer, Phys. Rev. Lett. **22**, 918 (1969).

[6]Y. Bouligand, J. Phys. (Paris), Colloq. **30**, C4-90 (1969).

[7]D. Schmidt, M. Shadt, and W. Helfrich, Z. Naturforsch. Teil A **27**, 277 (1972).

Submicrosecond bistable electro-optic switching in liquid crystals

Noel A. Clark [a] and Sven T. Lagerwall
Department of Physics, Chalmers Technical University, Goteborg, Sweden

(Received 3 March 1980; accepted for publication 13 March 1980)

Ferroelectric smectic *C* (FSC) liquid crystals are used in a simple new geometry that allows the spontaneous formation of either of two surface-stabilized smectic *C* monodomains of opposite ferroelectric polarization. These domains are separated by well-defined walls which may be manipulated with an applied electric field. The resulting electro-optic effects exhibit a unique combination of properties: microsecond to submicrosecond dynamics, threshold behavior, symmetric bistability, and a large electro-optic response.

PACS numbers: 61.30. – v, 78.20.Jq

In the smectic *C* (SC) liquid-crystalline phase molecules form a layered structure with the average orientation of the molecular long axes, denoted by the unit vector director $\hat{n}$ tilted at an angle Ω_0 to the layer normal ($\hat{z}$ axis). The director $\hat{n}$ exhibits a continuous degeneracy in its azimuthal orientation, lying on a cone coaxial with $\hat{z}$ (Fig. 1). The azimuthal orientation is thus readily manipulated by external forces or fields. Guided by an elegant physical argument, Meyer *et al.*[1] showed that, for suitably constructed chirally asymmetric molecules, the SC structue will be ferroelectric, with a macroscopic electric dipole density **P** locally normal to $\hat{n}$ and lying in the (x, y) plane of the layers. In principle, FSC's yield, as a result of **P**·**E** torques, a strong linear coupling of $\hat{n}$ to applied electric field **E**.[1,2] However, this linear coupling is eliminated on a macroscopic scale by an additional consequence of the molecular chirality, namely that $\hat{n}$ and **P** spiral about the $\hat{z}$ axis to form an effectively antiferroelectric helical structure. We demonstrate here that it is possible to use surface interactions to suppress the antiferroelectric helix in a geometry that simultaneously provides (i) the stabilization of either of two domains of opposite ferroelectric polarization separated by domain walls (a situation not permitted in the bulk because of the rotational degeneracy of $\hat{n}$); (ii) convenient **E** field selection of molecular orientation via domain-wall manipuation; (iii) a large optical response (equivalent to the rotation of a uniaxial dielectric of refractive index anisotropy $\Delta n \sim 0.2$ through an angle $2\Omega_0 \sim 45$).

Figure 1 illustrates the essential features of our geometry. The SC is confined between flat plates which are treated so that the director at a surface is constrained to lie in the plane of the surface ($\gamma_1 = 0$), but with no strong tendency for a particular orientation in the surface plane (γ_2 free). For samples having the layers normal to the plates, this boundary condition requires a disclinated texture in order to be

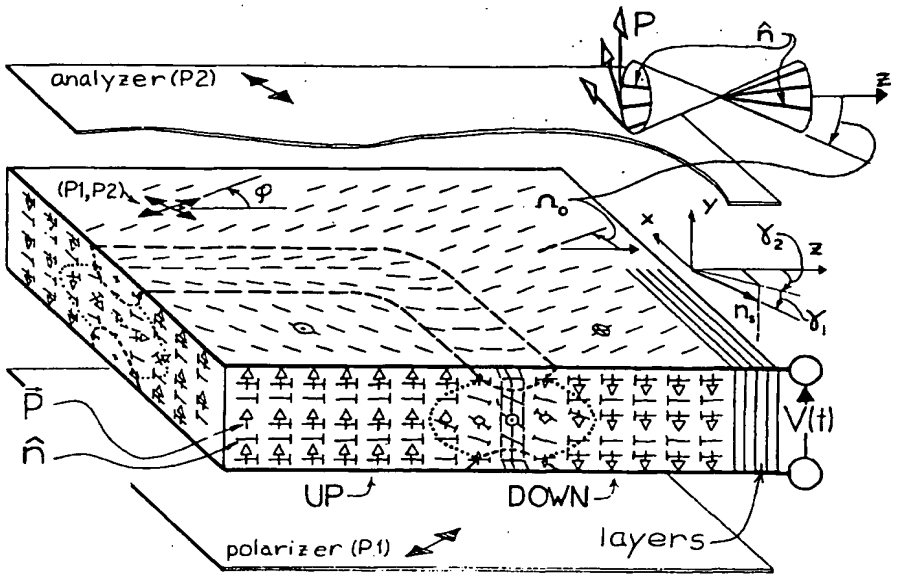

FIG. 1. Schematic of the sample geometry showing UP and DOWN domains and a domain wall (—| indicates a molecule whose right end projects outward). In the regions bounded by the dashed lines (-----) and the plates the SC tilt angle Ω is less than Ω_0. This represents the core of the disclination and, in fact, may be very small. There may also be small layer compression effects. The polarizer (P1) and analyzer (P2) are crossed, with the polarization direction at an angle φ to the $\hat{z}$ axis. For $\varphi = \Omega_0$, light traversing the polarizer-sample-analyzer sandwich will be extinguished in the DOWN state and transmitted in the UP state. A positive applied voltage moves the domain wall so that the DOWN region grows. Domain walls having the opposite helix sense are also possible and are observed.

[a] Permanent address: Dept. of Physics, Univ. of Colorado, Boulder, CO 80309.

 0003-6951/80/110899-03$00.50

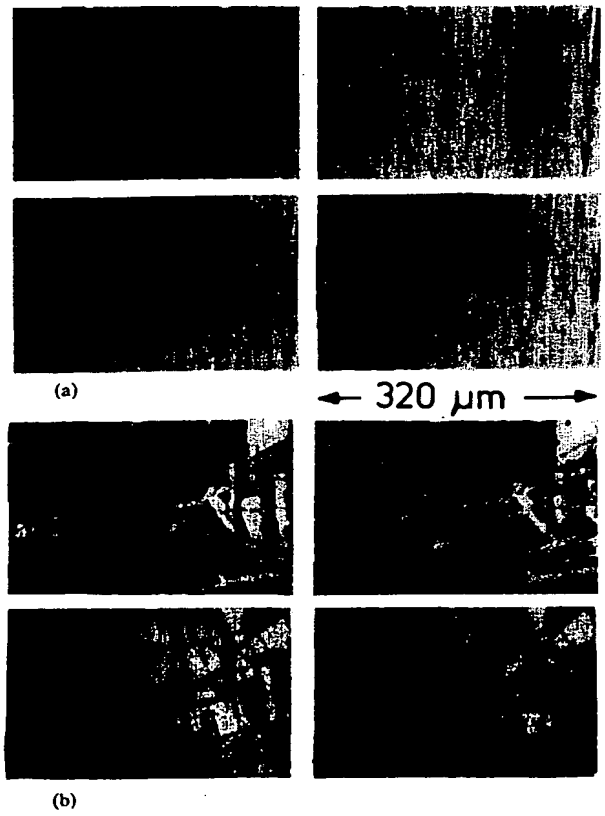

FIG. 2. Transmission micrographs (resolution $\sim 1\,\mu$m): (a) Domain-wall migration in a 1.5-thick SC DOBAMBC sample at $T = 84$ °C. The sample has been oriented by shear such that the layers are horizontal and normal to the page. The vertical texture is caused by remaining weak smectic layer undulations. The analyzer is horizontal and the polarizer is vertical making a small angle with the layer normal ($\varphi \simeq 1°$). Voltage sequence (left to right and down): 0, 0.5, 1.0, 1.5 V. The transmitted light contrast between UP (bright) and DOWN (dark) domains is evident. This contrast reverses as the sample is rotated through $\varphi = 0$ and at $\varphi = 0$ only the domain walls are visible, dark, and sharp on a light background. Note the closed domain-wall loops, indicating the presence of domain walls of both signs, and the coalescence of two loops to make one. (b) Sample appearance with $\varphi = \Omega_0$ under conditions of bistable operation. Vertical texture is as in 2(a), and horizontal lines are thin homeotropic regions resulting from the orienting shear. These serve to nucleate and terminate domain-wall motion. Voltage sequence: 1, (top left) −5 V; 2, (top right) 0 V; 3, (bottom left) +5 V; 4, (bottom right) 0 V.

compatible with the bulk $\hat{n}$, **P** helix. Since the energy required to unwind the helix decreases as the sample thickness d, this boundary condition will suppress the $\hat{n}$, **P** helix[3] for sufficiently thin samples ($d \lesssim P$, the helix pitch). In the absence of the helix there are two stable, equal energy configurations of the SC, illustrated in Fig. 1 for the idealized case of complete freedom of angle γ_2. For FSC's these two types of $\hat{n}$, **P** monodomains will possess opposite **P** normal to the plates, and will be denoted as the "UP "and "DOWN" states. The UP and DOWN states are structurally identical, differing only by a π rotation about the $\hat{z}$ axis (symmetric bistability). Adjacent UP and DOWN regions in a sample will be separated by well-defined domain boundaries (Fig. 1) which are π inversion walls in the $\hat{n}$, **P** field. The application of a field favoring the UP orientation produces torques in the wall which induce wall motion that expands the UP region and vice versa. Possible structures for domain walls parallel and normal to the SC layers are shown in Fig. 1. Note that the domains in our case are stabilized by surface mechanical forces and not by bulk forces, distinguishing it from that of crystalline ferroelectrics.

The optical effects associated with domain-wall motion arise from the different director orientations in the UP and DOWN states. Although weakly biaxial,[4] the SC may be taken for present purposes to be uniaxial, with the optic (high index) axis along $\hat{n}$. The simplest geometry has the sample between crossed polarizers with $\hat{n}$ parallel to the polarization direction in the DOWN state ($\varphi = \Omega_0$, Fig. 1) leading to extinction of light passing through the polarizers and sample (DOWN = OFF). In the UP state the polarization will make an angle $2\Omega_0$ with the optic axis and a fraction of the incident optical power F will be transmitted, with

$$F = F_0[\sin(4\Omega_0)\sin(\pi \Delta n\, d/\lambda)]^2.$$

Here Δn is the refractive index anisotropy, λ the vacuum optical wavelength, and F_0 the parallel polarizer transmis-

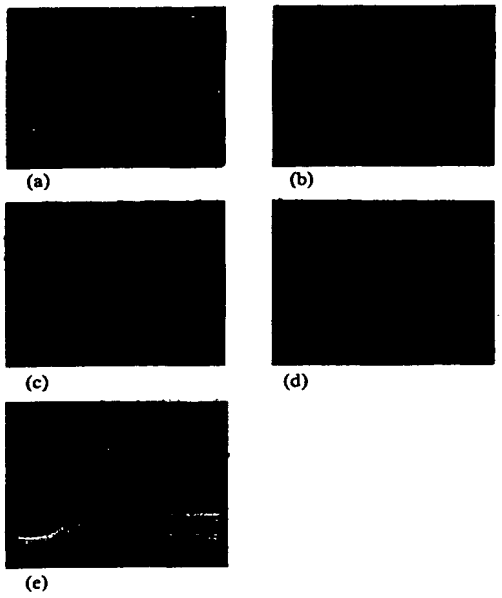

Fig. 3. Response of the optical transmission of a SC HOBACPC sample at $T = 68$ °C to pairs of opposite-polarity rectangular voltage pulses, spaced by 70 ms. VERT, photodiode output or applied voltage; HORIZ, time. (a) The top trace represents the optical response to above-threshold pulses showing switching to the OFF state at the beginning of the trace and back to the ON state 70 ms later. The ON pulses are above threshold for all traces. Top to bottom: response to OFF pulses of fixed width ($\tau = 1.4\,\mu$s) and variable amplitude $A = 44$, 37, 29, and 26 V (10 ms/div). (b) Photodiode response to OFF pulses of fixed amplitude ($A = 44$ V) and variable width: $\tau = 2.2$, 1.1, 0.9, and 0.6 μs (top to bottom), again the ON pulses are above threshold (10 ms/div). (c) Dynamic optical response showing applied pulse (top) and photodiode output (bottom): LEFT (2 μs/div): $A = 20$ V, $\tau = 2.0$ μs; RIGHT (1 μs/div): $A = 40$ V, $\tau = 1.0\,\mu$s. (d) Dynamic optical response showing a series of b actinic pulses (top) of varying width for which $A = 1.5$ V and $20 < \tau < 240\,\mu$s, and photodiode response (bottom); 50 μs/div. Traces have been displaced vertically to avoid overlap. For $A = 1.5$ V full latching occurs for $\tau > 200\,\mu$s.

sion. $F = F_0$ can be achieved for $\Omega_0 \gtrsim 23°$ [this condition is met for DOBAMBC[5] for $T \lesssim 85$ °C (Refs. 2, 4)], and $d > \lambda/2\Delta n$, implying $d > 2.5\lambda \sim 1.2\,\mu$m ($\Delta n \sim 0.2$ for DOBAMBC[4]).

We now turn to our experimental results. The bounding plates were glass, coated with semitransparent conductive ($100\,\Omega/\text{cm}^2$) SnO_2 layers. The SnO_2 surfaces were cleaned of contaminants and dust with spectrographic acetone and placed together without spacers (overlap area = 6×6 mm). The sample material was introduced between them by capillary suction from the isotropic phase, resulting in samples which were slightly wedged, typically varying from 0.5 to 3 μm in thickness. The compounds used in this study were optically active DOBAMBC[5] and HOBACPC.[5] Observations of the SA textures obtained upon cooling from the isotropic and obtained as a result of a gentle shearing of the bounding plates suggest the operative boundary conditions for these compounds to be those described above ($\gamma_1 = 0$, γ_2 free). The overall behavior of the two compounds was qualitatively similar except as noted below.

In the SC phase the helix was absent and the electro-optic response was characterized by the motion of resolution-limited domain walls separating regions having apparent optic axes (as determined by the angle φ of the crossed polarizer-analyzer required for extinction) oriented at angles $\varphi \sim \pm\,\Omega_0$ from the layer normal. The domain walls thus separate regions of nearly opposite polarization. Contrast ratios were limited by the degree of layer orientation achieved, with 20:1 typical over millimeter square areas for $|\varphi| = \Omega_0$.

Figure 2(a) shows typical domain-wall appearance in the SC phase. With a slowly varying voltage the detailed motion of the domain walls was followed and indicated their strong interaction with defects in the layer structure, surface imperfections and scratches, and subresolution defects. this observation prompted a search for bistable operation, which was indeed found, as indicated by Fig. 2(b), showing a sample in either the UP or DOWN state for zero applied field. Bistability was further studied by applying pairs of opposite polarity rectangular voltage pulses of selectable amplitude A, width τ, and time separation to the sample. The sample transmission was monitored by passing a 2-mW He-Ne laser through the microscope to a photodiode. Figure 3 shows typical results obtained on a 1.5-μm-thick[6] HOBACPC sample at $T = 68$ °C for pairs of pulses separated by 70 ms. Figures 3(a) and 3(b) show respectively the optical response to pulses of fixed width ($\tau = 1.4\,\mu$s and varying amplitude, and to pulses of fixed amplitude ($A = 44$ V) and varying width. For $A\tau$ sufficiently large, the optical response is bistable, with the (+ , −) pulse latching the monitored area ($200 \times 200\,\mu$m) into the (ON, OFF) state. The bistable latching exhibits a relatively sharp threshold, going from zero to saturated memory response for a less than 25% change in $A\tau$. The dynamic behavior of the optical response to a pulse [c.f. Fig. 3(c)] is characterized by a rise time τ_r which depends on pulse amplitude, increasing from a minimum of 1 μs for $A = 20$ V to 4 ms at $A = 0.2$ V. In general, for latching to occur, A and τ must be such that the saturated optical response is achieved during the applied pulse. An exception to this occurs for short, high-voltage pulses ($A > 20$ V) for which, although the optical response time does not decrease below 0.9 μs, it does exhibit "inertia," continuing to saturation after termination of the pulse. This minimum response time is comparable to the RC time constant of the sample sandwich. Full switching could be achieved with pulse widths τ_l over the range $A = 55$ V, $\tau_l = 500$ ns ($A\tau_l = 25$ V μs) to $A = 0.2$ V, $\tau_l = 4$ ms ($A\tau_l = 800$ V μs). This general trend and fast response is expected from the simplest theoretical estimate: $A\tau_l \sim \eta d/P \sim 10^{-4}$ V s, where is an orientational viscosity, although the predicted $\tau_l \sim A^{-1}$ dependence is obeyed only at the higher voltages ($A > 10$ V). The full response, once attained, was stable over periods of at least several hours. The dynamic response to fast-rise-time pulses was homogeneous (i.e., independent of the size L of the sample area monitored for $L > 5\,\mu$m), reflecting the nucleation and motion of many domain walls. Results in DOBAMBC were similar, with rise times and requisite pulse widths two to three times longer, presumably a result of the smaller value of P in this material.[7]

To conclude, the effects described here are of potential use where electro-optic effects having fast response and/or built-in memory are required (for example, matrix-addressed video display). This work was supported by the Swedish Natural Science Research Council and the Swedish Board of Technical Development.

[1]R. B. Meyer, L. Liebert, L. Strzelecki, and P. Keller, J. Phys. Lett. 36, L69–71 (1975).
[2]P. Martinot-Lagarde, J. Phys. (Paris) 37-C3, 129–132 (1976).
[3]The suppression of the helix for the stronger boundary condition $\gamma_1 = 0$, $\gamma_2 = \Omega_0$ to form a unique stable SC monodomain has been demonstrated [M. Brunet and C. Williams, Ann. Phys. 3, 237–248 (1978)].
[4]S. Garoff, Ph.D. thesis, Harvard University, 1977 (unpublished).
[5]DOBAMBC is decyloxybenzylidene p'-amino 2 methyl butyl cinnamate. See Ref. 1; HOBACPC is hexyloxybenzylidene p'-amino 2 chloropropyl cinnamate. See P. Keller, S. Juge, L. Liebert, and L. Strzelecki, C. R. A. S. 282C, 639-641 (1976). Both compounds have isotropic-SA-SC-SF phases.
[6]Sample thickness was determined using the Newton color sequence.
[7]P. Martinot-Lagarde, J. Phys. (Paris) Lett. 38, L17-19 (1977).